ARTICLE OPEN

Check for updates

Overexpressed transient receptor potential vanilloid 1 (TRPV1) in lung adenocarcinoma harbours a new opportunity for therapeutic targeting

Yichu Nie[1,2,7], Fenglan Feng[3,7], Wei Luo[1,7], Andrew J. Sanders[4], Yidi Zhang[2], Jiaming Liang[3], Cheng Chen[3], Weineng Feng[1], Weiquan Gu[1], Weiping Liao[5], Wei Wang[5], Jinfeng Chen[6], Lijian Zhang[6], Wen G. Jiang[4] and Jin Li[3]✉

The specific biological function of transient receptor potential vanilloid 1 (TRPV1) in pathogenesis of lung adenocarcinoma (LUAD) remains unclear. In this study, TRPV1 expression in tumor tissues, primary cells and cell lines of LUAD, as well as the mechanism mediating its hyperexpression were systematically studied. Multiple models and techniques were adopted to elucidate the relationship between TRPV1 hyperexpression and tumor recurrence and metastasis. Results showed that TRPV1 expression was increased in tumor tissues and primary tumor cells of LUAD patients. The increased expression was associated with worse overall survival outcome and raised HIF1α levels. TRPV1 expression in A549 and NCI-H292 cells was increased after pretreatment with cigarette smoke extract or spermine NONOate. Moreover, A549 cells with TRPV1 overexpression has enhanced tumor growth rates in subcutaneous grafted tumor models, and increased intrapulmonary metastasis after tail vein infusion in nude BALB/c nude mice. Mechanistically, TRPV1 overexpression in A549 cells promoted HIF1α expression and nuclear translocation by promoting CREB phosphorylation and activation of NOS1-NO pathway, ultimately leading to accelerated cell proliferation and stronger invasiveness. In addition, based on photothermal effects, CuS-TRPV1 mAb effectively targeted and induced apoptosis of TRPV1-A549 cells both in vivo and in vitro, thereby mitigating tumor growth and metastasis induced by xenotransplantation of TRPV1-A549 cells. In conclusion, TRPV1 hyperexpression in LUAD is a risk factor for tumor progression and is involved in proliferation and migration of tumor cells through activation of HIF1α. Our study also attempted a new strategy inhibiting the recurrence and metastasis of LUAD: by CuS-TRPV1 mAb precisely kill TRPV1 hyperexpression cells through photothermal effects.

Cancer Gene Therapy; https://doi.org/10.1038/s41417-022-00459-0

INTRODUCTION

Lung adenocarcinoma (LUAD) is the most commonly diagnosed histological subtype of non-small-cell lung cancer (NSCLC) and continues to present a clinical challenge due to the poor response to therapies and disappointing long-term survivals [1, 2]. Recently, for patients with specific mutations of EGFR [3], ALK [4, 5], RET [6], and ROS1 [7], molecular targeted therapies have improved the treatments. Meanwhile, novel targets like KRAS [8] and MET [9] are being studied. However, the complicated molecular patterns and high heterogeneity of LUAD limit the benefits of these targeted therapies to only specific patients, leaving a large number of LUAD patients without effective therapeutic drugs. Even antibodies against PD-1 are partly effective in treating patients with high expression of PD-L1, which improved overall survival [10, 11]. However, currently, cancer immunotherapy displays beneficial effects in less than 20% of patients [12]. Moreover, the high incidence of postoperative recurrence and metastasis are main causes for failure of treatment. The rapid progress in discovering molecules associated with disease progression and therapy resistance and understanding of mechanisms, would present new opportunities to reveal new promising therapy targets, and hopefully reduce the recurrence rate and improve the survival rate.

Transient receptor potential vanilloid 1 (TRPV1) is a cation channel protein affiliated to a member of the six non-selective cationic channel protein family, which existed on the cell membrane or intracellular organelle membrane and are highly selective for calcium transportation [13]. TRPV1 was shown widely distributed in both central nerves such as hippocampus and synapses, and peripheral sensory nerve endings. It can be activated by heat (greater than 43 °C), cannabinoid, acids, and osmotic pressure changes. Activation of TRPV1 plays a role in synaptic transmission, temperature regulation, pain modulation and apoptosis regulation [14–16]. This TRPV member, amongst all the family members is now known to be expressed more abundantly in other non-neural tissues including lung tissues,

[1]Clinical Research Institute, The First People's Hospital of Foshan & Sun Yat-sen University Foshan Hospital, Foshan 528000, PR China. [2]School of Pharmaceutical Sciences (Shenzhen), Sun Yat-sen University, Guangzhou 510275, PR China. [3]State Key Laboratory of Respiratory Diseases, the First Affiliated Hospital of Guangzhou Medical University, Guangzhou Medical University, Guangzhou 510120, PR China. [4]CCMRC, Cardiff University School of Medicine, Cardiff, UK. [5]Foshan Fourth People's Hospital, Foshan 528000, PR China. [6]Peking University Cancer Hospital and Beijing Cancer Institute, Department of Thoracic Surgery, Fucheng Road, Haidian District, Beijing, China. [7]These authors contributed equally: Yichu Nie, Fenglan Feng, Wei Luo. ✉email: JinL@gzhmu.edu.cn

Received: 21 September 2021 Revised: 26 February 2022 Accepted: 9 March 2022
Published online: 30 March 2022

compared with the other 5 members, which are more confined to nerve tissues [17]. Recently, we and others have found that TRPV1 is present in a diverse range of cancer cells and cancer tissues [18, 19]. Zhu et al. reported that TRPV1 expression was increased in LUAD patients after lung cancer surgery [18]. Moreover, our previous study had confirmed that the expression of TRPV1 and TRPA1 in A549 cells (a cell line collected from a LUAD patient) was upregulated after HIF1α activation [19]. TRPV1 has otherwise been reported to be associated with the regulation of tumor growth, neurogenesis, cancer pain and possibly disease progression of malignancies [20, 21]. Although TRPV1 has been widely confirmed to regulate apoptosis and synaptic development, it is not clear whether it is involved in regulating postoperative recurrence and metastasis of cancer cells in human LUAD in clinical settings and indeed if it has any value for therapeutic targeting.

RhoA, Rac1, and Cdc42 are key regulatory factors of tumor invasion and metastasis by regulating cell morphology change, cell-matrix adhesion and cytoskeletal recombination [22]. Previous studies have demonstrated that the transcription of these genes is mainly promoted by hypoxia-inducible factor 1α (HIF1α) nuclear accumulation, which would be activated by endogenous NO or NO donors even if under normoxic conditions [23]. Considering that both TRPV1 and calcium-dependent neural nitric oxide synthase (nNOS) are expressed in tumor cells of LUAD patients, we hypothesized that there exists a TRPV1-Ca^{2+}-nNOS-NO signaling pathway that enhances proliferation and metastasis in these tumor cells by activating HIF1α. It leads to further suggestion that tumor cells with high expression of TRPV1 in LUAD patients are more aggressive with high invasion and metastatic activity. Should this hypothesis be correct, it would allow the development of new photothermal nanomaterials targeting TRPV1, in order to accurately locate TRPV1 hyper-expression tumor cells and reduce/eliminate TRPV1 mediated invasion and metastasis in vitro and in vivo.

To explore the possible role of TRPV1 in tumor postoperative recurrence and metastasis of LUAD, first we determined TRPV1 and HIF1α expression in multiple lung cancer cells including A549 cells and clinical tissue samples from LUAD patients who underwent lobectomy of the lung. Second, we verified the cross-talk and potential mechanisms between TRPV1 and HIF1α in promoting tumor proliferation and metastasis of LUAD both in vitro and in vivo. Finally, we assessed the cytotoxicity and targeting accuracy of CuS-TRPV1 mAb to TRPV1 hyper-expression tumor cells in vitro and evaluated its inhibitory effect on tumor proliferation and metastasis using in vivo mice xenotransplantation models.

MATERIALS AND METHODS

Detailed experimental materials, methods, and procedures are given in the Supplementary Materials.

Patients and clinical specimens

The study used two lung cancer cohorts. The first eight pairs was prospectively collected Non-small cell lung cancer and background tissues. This small cohort was used as pilot study. The second cohort had a total of 383 tumor samples and normal lung tissue samples, obtained from patients who were enrolled between 2004 and 2007. The tissues were obtained immediately after resection of lung tumors. The following was excluded from the collection: patients with chemotherapies or radiotherapies prior to surgery and patients with family history of cancers. Patients who were lost during the follow up was also subsequently excluded. The median age of the patient cohort was 61 years of age (range from 39 to 74 years). The gender distribution between the patients were 69% male and 31% female. All of the human specimens and data were obtained according to a protocol reviewed and approved by the local ethical committee, and all patients signed an informed consent form. Detailed demographic information for all patients involved in this study is shown in Supplementary Tables S1 and S2.

Analysis of TRPV1 expression and its correlation with clinical characteristics

Real-time PCR for TRPV1 and β-actin was performed with an ABI Prism 7900 System (Applied Biosystems) using the Absolute Q-PCR ROX Mix (Thermo Fisher Scientific, Waltham, MA, USA). The transcript copy number of TRPV1 was determined by absolute quantification following a previously reported method [24, 25] using J probe (patent number: 201810845605.9). The expression level was calculated based on an internal standard, β-actin. Correlations between TRPV1 levels and demographical features were assessed using Mann–Whitney rank sum and Kruskal–Wallis one-way analysis of variance tests. Kaplan–Meier survival curves and log-rank tests were used to evaluate differences in OS.

Histological evaluation and immunohistological/immunofluorescence analyses for TRPV1 and HIF1α

Normal lung tissues, LUAD cancer tissues and lymphatic tissues were paraffin-embedded and stained by the procedures previously described [26].

In vitro studies

Cells, cell transfection, and gene expression interference. A549 cells were maintained according to the supplier's instructions. TRPV1-A549 cells were constructed by transfecting A549 cells with the lentiviral expression vector pEZ-Lv206 containing full-length complementary DNA of human TRPV1, green fluorescent protein (GFP) and puromycin resistance genes. TRPV1 siRNA or HIF1α siRNA transfection into A549/TRPV1-A549 cells was performed using the method described previously [19]. The proliferation and migration of A549/TRPV1-A549 cells influenced by TRPV1 siRNA (5 nM, for 48 h), HIF1α siRNA (5 nM, for 48 h), or CPZ (25 μM, for 1 h) were detected by MTT assay and Transwell migration assay, respectively.

Western blot analysis. Cytoplasmic expressions of TRPV1, MMP1, MMP9, RhoA, Rac1, Cdc42, Cyclin A2, PCNA, CaKMII, phospho-CaKMII, cyclic-AMP response element-binding protein (CREB), phospho-CREB, nNOS, and β-actin, as well as intracellular HIF1α and Histone, were detected by Western blot. Protein band intensities were visualized and digitized using Image J software.

Immunocytochemical (ICC) staining. HIF1α expression and nuclear translocation influenced by TRPV1 siRNA (5 ng mL^{-1}, for 48 h) or CAP (10 ng mL^{-1}) were detected by ICC staining. The nucleus of cells was counterstained with DAPI before visualizing on a fluorescent microscope.

NO production and quantitation. Intracellular NO production was assessed using DAF-FM DA probe following to the method published previously [27]. CAP (10 nM, dissolved in PSS) was applied for 3 min to assess CAP-induced NO production. For the compound test, cells were pre-superfused with CPZ (25 μM), L-NAME (25 μM), NEM (25 μM), or ODQ (25 μM) for 10 min, and then superfused with solutions containing CAP (10 nM) for 3 min.

Intracellular calcium influx. Calcium influx ($[Ca^{2+}]_i$) was measured by Fura-2 AM in TRPV1-A549 cells according to the method described previously [28]. CAP (10 μM, dissolved in PSS) was applied for 3 min to show $[Ca^{2+}]_i$ in TRPV1-A549 cells. For the compound test, cells were pre-superfused with CPZ (25 μM), L-NAME (25 μM), NEM (25 μM), or ODQ (25 μM) for 10 min, and then superfused with solutions containing CAP (10 nM) for 3 min.

CuS-TRPV1 mAb Synthesis and characterization. CuS-TRPV1 mAb was synthesized by the method previously published [29]. Briefly, citrate-capped CuS nanoparticles were synthesized and then the carboxylate groups of the particles were activated by EDC and NHS. CuS-TRPV1 mAb nanoparticles were synthesized by coupling the carboxyl groups on the citrate-capped CuS with the amino groups of TRPV1 antibody to form the amido bonds.

Cytotoxicity tests of CuS-TRPV1 mAb. A549 and TRPV1-A549 cells were seeded and then incubated with CuS-TRPV1 mAb (0.4 mg mL^{-1}) for 2 h. The CuS-TRPV1 mAb groups were then irradiated with a 980 nm laser (1.0 W cm^{-2}) for multiple times (1, 10, 20, and 30 cycles). Cell viability was evaluated by MTT assay.

Cellular localization experiment to test the targeting property of CuS-TRPV1 mAb. Intracellular localization of CuS-TRPV1 mAb was monitored using immunofluorescence method. The APC-conjugated CuS-TRPV1 mAb

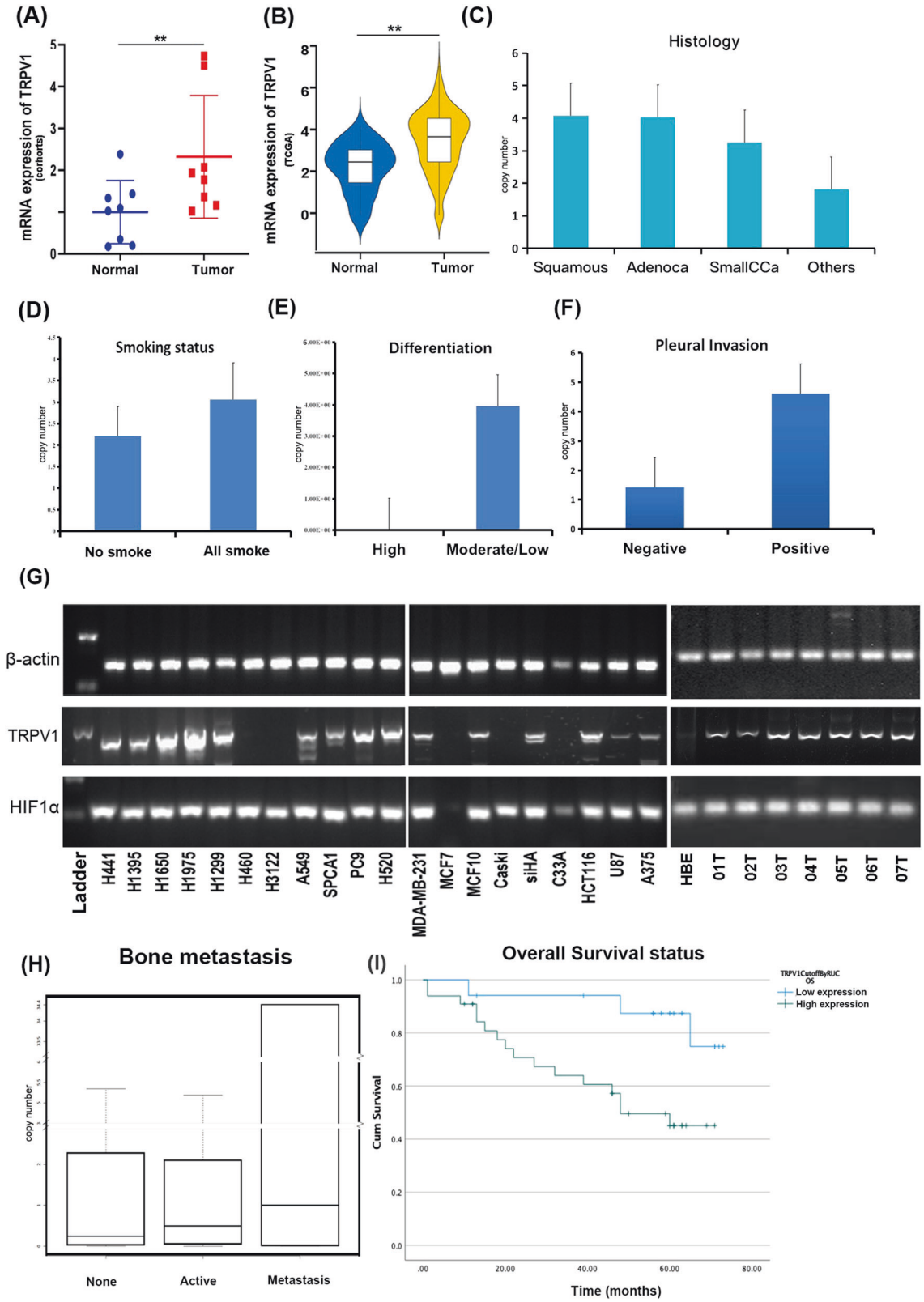

(0.4 mg mL^{-1}) was respectively cultured with A549 or TRPV1-A549 cells for 2 h. Cell images were acquired under a fluorescence microscope. The green fluorescence of GFP reflected cells with high expression of TRPV1, while the red fluorescence of APC reflected the captured CuS-TRPV1 mAb in A549 cells or TRPV1-A549 cells.

In vivo tumor models

Tumor xenograft growth assays. Male BALB/c nude mice (5–6 weeks old) were subcutaneously injected with stable TRPV1-A549 cells or A549 cells (1×10^6 cells per mice) for tumor establishment. Based on the Lehr's power prediction method and our previous in vivo studies, we included 5 subject

Fig. 1 TRPV1 expression was increased in LUAD patients, especially in patients with worse overall survival outcome. (**A**) TRPV1 mRNA expression was determined in 8 paired tumor and normal tissues of LUAD patients ($P = 0.0399$). (**B**) Boxplots constructed by data downloaded from TCGA showed the validation of expression of TRPV1 mRNA in lung adenocarcinoma (LUAD)and background ($P < 0.0001$). TRPV1 transcription levels were determined in (**C**) squamous cell carcinoma [Squamous, Mean ± SE: 4.07 ± 0.24, $n = 32$], adenocarcinoma [Adenoca, Mean ± SE: 4.02 ± 0.08, $n = 40$], small cell carcinoma [SmallCCa, Mean ± SE: 3.247 ± 0.8, $n = 3$] and other histological types [Others, Mean ± SE: 1.81 ± 1.4, $n = 3$]; (**D**) patients without smoking habit [Mean ± SE: 2.203 ± 0.7, $n = 61$], and smokers [Mean ± SE: 3.061 ± 0.8, $n = 77$, $P = 0.44$]; (**E**) tumors of high differentiation [Mean ± SE: 0.34 ± 0.25, $n = 16$], and low or moderate differentiation [Mean ± SE: 4.46 ± 1.4, $n = 49$, $P = 0.0044$]; (**F**) in patients with pleural invasion [positive, Mean ± SE: 4.62 ± 2.75, $n = 18$], and with negative pleural invasion [negative, Mean ± SE: 1.42 ± 1.06, $n = 9$]. (**G**) The mRNA expressions of TRPV1 and HIF1α in 20 cancer cell lines and 7 primary cancer cell lines were verified by RT-PCR. (**H**) The box plot showed TRPV1 transcription levels in patients without metastasis [None, Median: 0.248, interquartile range (IQR) 2.265, $n = 93$], with radio-active sites [Active, Median: 0.49, IQR: 2.06, $n = 39$] and with bone metastasis [Metastasis, Median:1.0, IQR: 34, $n = 3$]. (**I**) Kaplan–Meier survival curves show the overall prognosis of patients with low TRPV1 expression ($n = 11$) and high TRPV1 levels ($n = 10$) based on log-rank tests. Data were expressed as Mean ± SEM ($n = 8$). *Represents significant difference as compared with control group, *$p < 0.05$, **$p < 0.01$.

in each of the study groups. The mice in TRPV1-A549 + CuS-TRPV1 mAb group were intravenously administered with CuS-TRPV1 mAb nanoparticles at a concentration of 10 mg kg^{-1}, while the mice in TRPV1-A549 cells group received the same volume of PBS. The mice were then irradiated using NIR laser 2 h, post CuS-TRPV1 mAb nanoparticles injection (980 nm, 5 W/cm^2, spot diameter size 0.5 cm), at the cardiac region for 30 cycles. Tumor diameters were measured every 4 days to calculated tumor volumes. On day 28, the mice were sacrificed and the excised tumors were weighed and then fixed for H&E and IHC staining.

Tumor metastasis assays. Male BALB/c nude mice (5–6 weeks old, $n = 5$) were injected with TRPV1-A549 cells or A549 cells (1×10^6 cells per mice) via tail vein, followed by pretreatment with CuS-TRPV1 mAb (0.4 mg mL^{-1}), and irradiated with a 980 nm laser (1.0 W cm^{-2}) for 10 cycles. The mice were sacrificed at 35 days post-injection. Lungs were excised to evaluate the presence and number of metastatic nodules and then fixed for H&E staining.

Statistical analysis

All the analyses were performed using Statistical Software R version 4.0.0 or SPSS. Statistical significances were analyzed by the two-tailed unpaired Student's *t*-test; *P*-values of less than 0.05 were considered statistically significant in all statistical analyses. The correlation relationship between the expression level of HIF1α and TRPV1 was calculated using Pearson correlation. Wilcoxon test was performed to compare the expression level of TPRV1 in different stages, tumor size, lymph node metastasis status, and distant metastasis status in LUAD. Student's *t*-test was performed to analyze the difference between the TPRV1 expression in clinical LUAD patients' normal and tumor samples. For survival analysis, log-rank test was performed to test the difference in the Kaplan–Meier survival plot.

RESULTS

TRPV1 expression is upregulated in NSCLC tumors

As shown in Fig. 1A, we firstly analyzed TRPV1 mRNA expression in 8 LUAD paired samples (including tumor tissue and adjacent non-tumor tissue from the same patient) and found that TRPV1 mRNA expression in LUAD tumor tissues was significantly increased compared with non-tumor tissue ($P < 0.01$; Fig. 1A). The trend was validated according to TCGA database, the levels of TRPV1 expression in tumor tissues of LUAD patients were also significantly higher than in normal tissues ($P < 0.01$), with the median value of 3.81 (inter-quartile range (IQR) 2.59–4.70) in tumor tissues versus 2.59 (IQR 1.59–3.17) in normal tissues (Fig. 1B).

We next analyzed the transcript level of TRPV1 (copy numbers) based on a panel of cohorts including 383 tumor samples and normal lung tissue samples. The expression level of TRPV1 was analyzed in association with the clinical characteristics. The expression of TRPV1 was mainly distributed in adenocarcinoma and squamous cell carcinoma, compared with other histology subtypes (Fig. 1C). There was a trend that the transcript level of TRPV1 was higher in smokers (Fig. 1D), which might be related to the stimulation of hypoxia and HIF1α.

Increased TRPV1 expression is associated with metastasis and poor prognosis

Interestingly, the expression level of TRPV1 in patients with high differentiation was significantly lower compared with the patients who developed low or moderate differentiation tumors, which indicated a higher degree of malignancy. The cell line screening was carried out on a panel of cancer cell lines including lung cancer, breast cancer, cervical cancer, and other cancer types. The results showed TRPV1 was widely expressed in lung cancer cells, and partly shown in breast cancer and colon cancer cells. The TRPV1 expression was further determined in primary cancer cells which were derived from NSCLC patients we collected during 2021 in our clinical center. Compared with the HBE (human bronchial epithelial cells) where the TRPV1 was barely detected, the expression of TRPV1 was significantly seen in primary cancer cells derived from patients with clinical stage higher than IA (Fig. 1G, T03-T07). Among the early stage patients, a weak expression pattern of TRPV1 was shown in Cis (01 T) and patients with tumors smaller than 1 cm^3 (diameter ≤0.8) (02T) The transcript level of TRPV1 was further found to be associated with metastasis. The expression level of TRPV1 in patients who developed pleural invasion (4.62 ± 2.75, Mean ± SE) was higher than in the patients with no pleural invasion (1.42 ± 1.06, Mean ± SE), however, the *p*-value didn't reach statistical significance. Compared with the patients who had no metastatic diseases, the TRPV1 level was observed higher in patients who developed distant bone metastasis ($P = 0.05$) (Fig. 1H). The trends did not reach statistical significance which may due to the degree of variance caused by small sample volume of metastasis positive patients.

There is no statistical difference of levels of TRPV1 between male and female patients ($p = 0.674$ by Mann–Whitney test or $p = 0.608$ by non-paired *t* test). There does not appear to be a significant correlation between age and the levels of TRPV1 ($r = 0.135$, $p = 0.325$ by Spearman correlation test, or $r = 0.136$, $p = 0.336$ by Pearson correlation test

Survival rates were compared between patient groups defined by using median TRPV1 expression level as a cut-off threshold. Patients with tumors expressing lower levels of TRPV1 had longer overall survival (OS, median = 66 months; 95% CI, 59.1–74.1 months), compared with the OS of patients with tumors expressing higher TRPV1 expression (median = 46 months; 95% CI, 37.9–56.0 months), (Fig. 1I; $P = 0.014$). In addition, the effect of TRPV1 expression remained highly significant in correlation with overall survival after adjustments for age, sex, smoking status and clinical stage, suggesting that TRPV1 can be an independent prognostic predictor (Supplementary Table S1).

The positive correlation of TRPV1 expression and HIF1α

We further explored the correlation between TRPV1 and HIF1α in the TCGA cohort and found a significant correlation between increased TRPV1 and increased HIF1α levels ($R = 0.16$, $P < 0.01$; Fig. S1). This led to analysis of protein levels of TRPV1 and HIF1α in 8 LUAD sample pairs which, in addition to the matched tumor and

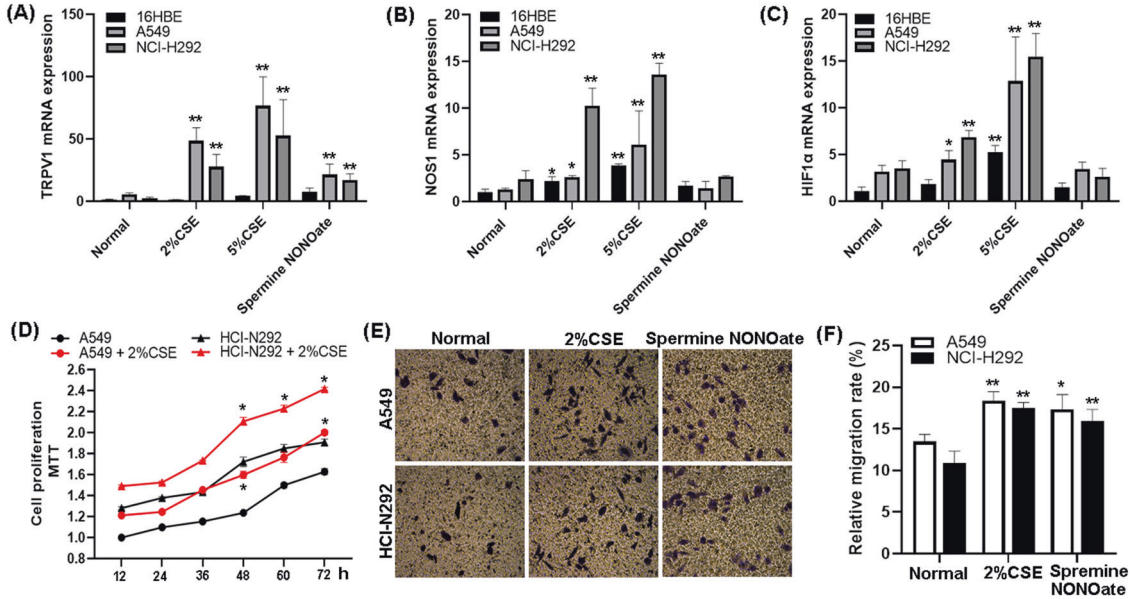

Fig. 2 CSE and Spermine NONOate pretreatment increased the mRNA expressions of TRPV1, NOS1, and HIF1α in A549 cells and NCI-H292 cells, as well as promoted cells proliferation and migration. 16HBE, A549, and NCI-H292 cells were cultured with FBS-free medium containing cigarette smoke extract (CSE, 2% or 5%) or Spermine NONOate (100 μM) for 6 h. Then the mRNA expressions of TRPV1 (**A**), NOS1 (**B**), and HIF1α (**C**) in 16HBE, A549, and NCI-H292 cells were measured by qPCR. (**D**) A549 and NCI-H292 cells were cultured up to 72 h with FBS-free medium containing 2% CSE or not, then cells proliferation rate was tested by MTT. (**E**), (**F**) The migration rate of A549 and NCI-H292 cells influenced by 2%CSE (24 h) or Spermine NONOate (100 μM, for 24 h) was tested by trans-well migration assay. Data were expressed as Mean ± SEM ($n = 3$). *Represents significant difference as compared with control group, *$p < 0.05$, **$p < 0.01$.

normal tissues, had lymphatic tissues from the same patients stained by IHC and IFC (Fig. S2). HIF1α staining was mainly located in the nucleus of tumor cells, whereas TRPV1 positive staining was mainly seen on the membrane of tumor cells. Moreover, the expression of TRPV1 and HIF1α were significantly upregulated both in tumor tissues and lymph nodes, as compared with the adjacent normal tissues ($P < 0.05$) (Fig. S2A). We also discovered with interest that lymphatic tissue in the tumors had a significantly higher level of TRPV1 (Fig. S2B) and HIF1α (Fig. S2C), than in normal tissues.

TRPV1 expression in both A549 and NCI-H292 cells was increased after cigarette smoke extract (CSE) or NO donor spermine NONOate pretreatment

As shown in Fig. 2A–C, TRPV1 was constitutively expressed in 16HBE, A549 and NCI-H292 cells, with higher expression levels in both LUAD cell lines A549 and NCI-H292 than that in 16HBE cells. Moreover, the expression of TRPV1 in A549 and NCI-H292 cells was significantly increased after pretreatment with cigarette smoke extract (CSE, 2% or 5%) or spermine NONOate (100 μM) for 6 h, while only CSE pretreatment could markedly increase the expression of NOS1 and HIF1α. As shown in Fig. 2D, 2%CSE significantly promoted the proliferation rate of A549 and NCI-H292 cells, while Spermine NONOate had no effect on proliferation of these cells (data not show). In addition, the migration rate of A549 and NCI-H292 cells was significantly promoted after pretreatment with 2%CSE or Spermine NONOate (100 μM) (Fig. 2E, F). These results suggested that CSE and NO have different mechanisms in inducing cell proliferation and migration, and the role of TRPV1 in the proliferation and migration of LUAD cancer cells is worthy of further ascertaining.

TRPV1 overexpression enhanced the proliferation and metastasis rates of A549 cells after xenotransplantation into BALB/c nude mice

In the in vivo tumor subcutaneous xenograft models, TRPV1-A549 cells or A549 cells (1×10^6 cells per mice) were injected into the left dorsal flank of the respective groups. The results from Fig. 3A and B showed that tumors formed by TRPV1-A549 cells were grew significantly faster and yielded significantly larger tumors at the conclusion (with tumor volume of 0.157 cm^3 versus 0.095 cm^3, $P < 0.05$). IHC staining of the resected tumors confirmed that tumors formed by both TRPV1-A549 cells and A549 cells contained abundant number of CK7 and Ki67 positive cells, indicating that the cells survived and proliferated after transplantation (Fig. 3C). ICC staining of the resected tumors confirmed that the expressions of TRPV1 and HIF1α in tumors formed by TRPV1-A549 cells were significantly higher than that in tumors formed by A549 cells ($P < 0.01$; Fig. 3D, E).

In the systemic metastasis model established by tail vein injection of A549 cells or TRPV1-A549 cells (BALB/c nude mice), mice were sacrificed at 35 days post-injection and the metastatic nodules formed in the lungs were calculated. There was a significantly increased number of metastatic nodules in the TRPV1-A549 cells injection group as compared with the A549 cells injection group (47.0 ± 17.3 versus 21.3 ± 5.6; $P < 0.01$; Fig. 3F, G).

TRPV1 overexpression rendered rapid growth and increased invasiveness in lung cancer cells

Since TRPV1 overexpression improved the proliferation rate of A549 cells after subcutaneous transplantation in mice, whether blocking TRPV1 expression by siRNA could attenuate the proliferation of A549 cells has been evaluated. As shown in Fig. S3, after treatment with 4 kind of TRPV1 siRNA sequences for 48 h, the expression level of TRPV1 in A549 cells was decreased by 1.2%, 21.7%, 62.8%, or 55.6%, respectively. siRNA3 (Assay ID 7691, 1.5 μg/mL Thermofisher) showed the strongest inhibition of TRPV1 expression in A549 cells. Therefore, this sequence was selected as the TRPV1 siRNA to carry out subsequent studies. TRPV1-A549 cells exhibited increasing proliferation rates, as compared with A549 cells pre-incubated with TRPV1 siRNA, or TRPV1-A549 cells pretreated with CPZ (25 μM) (Fig. 4A). Concurrently, the expressions of Cyclin A and PCNA in TRPV1-A549 cells were markedly higher than in A549 cells pre-incubated with TRPV1 siRNA

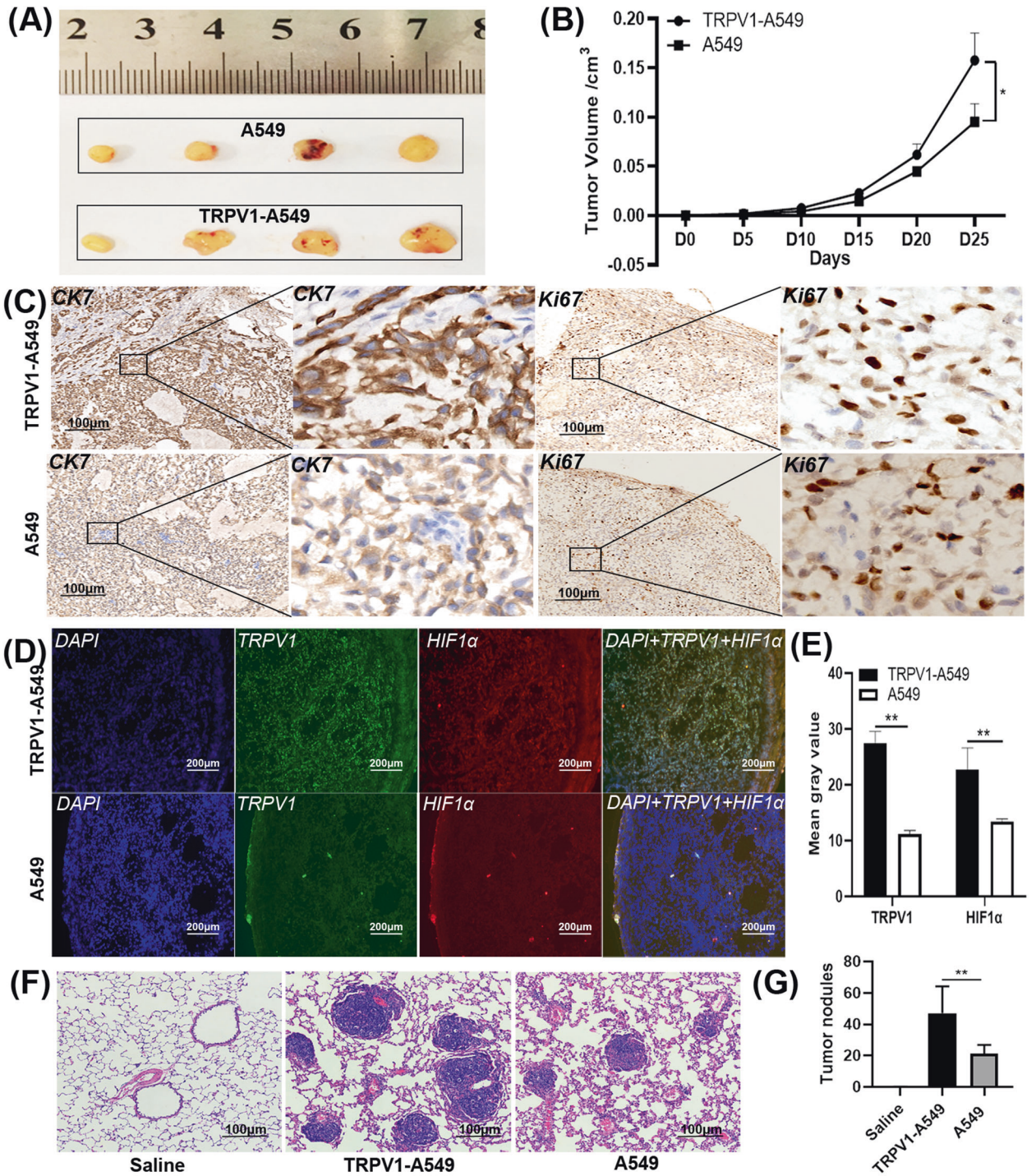

Fig. 3 TRPV1 overexpression enhanced the proliferation and metastasis rate of A549 cells after xenotransplantation into BALB/c nude mice. (**A**) Subcutaneous tumors were harvested from BALB/c nude mice transplanted with A549 or TRPV1-A549 cells. (**B**) Tumor volume changes after transplantation with A549 or TRPV1-A549 cells. (**C**) CK7 and ki67 expression in subcutaneous tumors. IFC staining (**D**) and quantitative analysis (**E**) of TRPV1 and HIF1α in subcutaneous tumors. (**F**) H&E staining showing metastatic nodules of systemic metastasis established by tail vein injection of A549 cells or TRPV1-A549 cells. (**G**) Quantitative number of metastatic nodules induced by the TRPV1-A549 or A549 cells tail vein injection. Data were expressed as Mean ± SEM ($n = 5$). *represents significant difference as compared with control group, *$p < 0.05$, **$p < 0.01$.

($P < 0.01$; Fig. 4B). In addition, CPZ (25 μM) pretreatment tended to, but not significantly, decrease the expressions of both Cyclin A and PCNA in TRPV1-A549 cells ($P > 0.05$; Fig. 4B).

TRPV1-A549 cells were more motile than the same cells pre-incubated with TRPV1 siRNA or CPZ (25 μM) ($P < 0.01$; Fig. 4C, D). As shown in Fig. 4E, F, the expressions of 5 tested invasive surrogate markers (RhoA, Rac1, Cdc42, MMP1, and MMP9) in TRPV1-A549 cells were slightly, but not significantly, increased than in A549 cells. Moreover, TRPV1 siRNA pretreatment reduced the expressions of the 5 surrogate invasive markers (Fig. 4E, F).

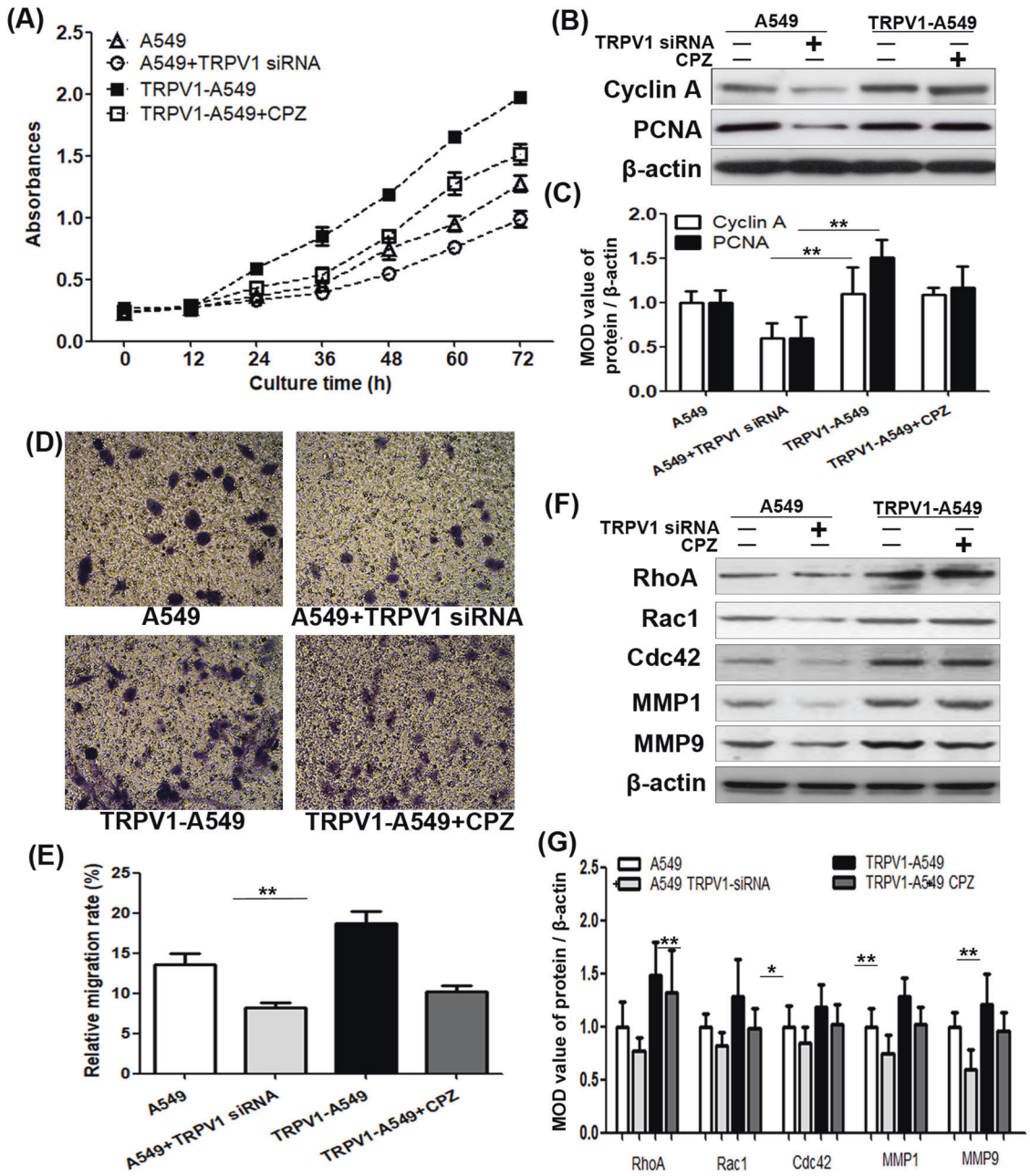

Fig. 4 TRPV1 overexpression promoted rapid growth and invasiveness in lung cancer cells. (**A**) The proliferation of A549 or TRPV1-A549 cells influenced by TRPV1 siRNA (5 nM, for 48 h) or CPZ (25 μM, for 1 h) was detected by MTT assay. (**B**) Cytoplasmic cyclin A and PCNA expression influenced by TRPV1 siRNA or CPZ were measured by western blot. (**C**) The Mean Optical Density (MOD) of bands for Cyclin A and PCNA were visualized and analyzed using Image J software. (**D**), (**E**) The migration of A549 or TRPV1-A549 cells influenced by TRPV1 siRNA or CPZ was detected by trans-well migration assay. (**F**) Cytoplasmic MMP1, MMP9, RhoA, Rac1, and Cdc42 expression influenced by TRPV1 siRNA or CPZ were measured by western blot. (**G**) The MOD value of MMP1, MMP9, RhoA, Rac1, and Cdc42 were visualized and analyzed using Image J software. Data were expressed as Mean ± SEM ($n = 3$). *Represents significant difference as compared with control group, *$p < 0.05$, **$p < 0.01$.

HIF1α is a key mediator in TRPV1 induced cell growth and invasion in lung cancer cells

HIF1α mRNA expression was elevated significantly in both A549 cells and TRPV1-A549 cells after 1 h incubation in medium with CAP (10 nM) (Fig. 5A). Moreover, TRPV1 siRNA (5 nM) pretreatment blocked CAP-induced HIF1α mRNA hyperexpression in both A549 cells and TRPV1-A549 cells, arguing that the CAP-induced hyperexpression of HIF1α mRNA was potentially mediated by TRPV1 activation. To test this possibility, TRPV1 antagonist CPZ and CaMKII inhibitor KN93 were used to block the downstream signaling pathway of TRPV1. It was shown that HIF1α mRNA expression induced by CAP was significantly reduced in TRPV1-A549 cells pretreated with CPZ (25 μM) or KN93 (25 μM) (Fig. 5B). It was also noteworthy that CAP (10 nM) stimulated a significant increase in phosphorylation of both CaMKII and CREB in TRPV1-A549 cells (increased to 3.3- and 2.8- fold, respectively), which were partially inhibited by CPZ or KN93 pretreatment (Fig. 5C, D). We further demonstrated that the growth and invasion of TRPV1-A549 cells were blocked by pretreatment with HIF1α siRNA (5 nM) for 48 h (Fig. 5E, F). These results collectively suggest that TRPV1 induced proliferation and invasion of A549 cells is mediated, at least in part, by upregulating expression of HIF1α.

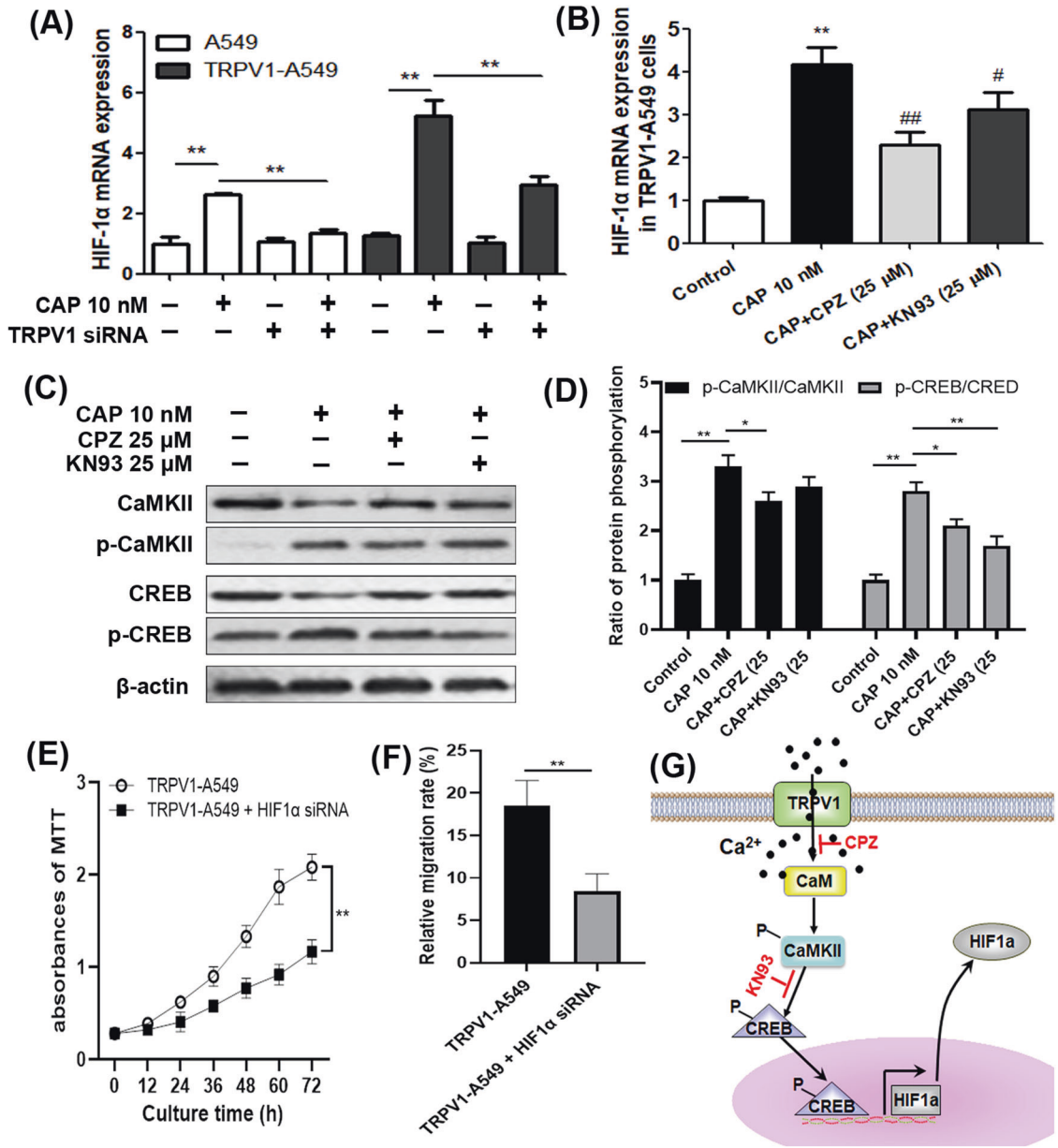

Fig. 5 HIF1α is a key mediator in TRPV1 induced cell growth and invasion in lung cancer cells. (**A**) HIF1α mRNA expression in both A549 cells and TRPV1-A549 cells after incubation in medium with CAP (10 nM, 1 h) or HIF1α siRNA (5 nM, for 48 h) was detected by RT-PCR. (**B**) HIF1α mRNA expression in TRPV1-A549 cells after incubation with CAP (10 nM, 1 h), CPZ (25 μM, for 1 h), or KN93 (25 μM, for 1 h) was detected by RT-PCR. (**C**) Cytoplasmic expressions of CaKMII, p-CaKMII, CREB, and p-CREB influenced by CAP, TRPV1 siRNA, or CPZ was measured by western blot. (**D**) Ratio of protein phospohorylation including p-CaKMII/CaKMII and p-CREB/CREB was quantitatively analyzed based on the Mean Optical Density (MOD) of bands from western blot. (**E**) The proliferation of TRPV1-A549 cells influenced by HIF1α siRNA (5 nM, for 48 h) was detected by MTT assay. (**F**) The migration of TRPV1-A549 cells influenced by HIF1α siRNA was detected by trans-well migration assay. (**G**) Proposed mechanism and signal pathway involved in TRPV1-induced HIF1α mRNA expression. Data were expressed as Mean ± SEM ($n = 3$). *Represents significant difference as compared with control group, *$p < 0.05$, **$p < 0.01$.

TRPV1 overexpression promotes HIF1α nuclear translocation through activation of NOS1-NO pathway

HIF1α is known to regulate gene transcription when translocated into the nucleus. This was demonstrated in our cell models, in that the staining of HIF1α (stained in red) was much stronger in the cytoplasm of TRPV1-A549 than in TRPV1 siRNA pretreated cells. Moreover, treating the TRPV1-A549 cells by CAP (10 nM) significantly increased positive staining of HIF1α in the nucleus, but not in the nucleus of TRPV1 siRNA pretreated cells (Fig. 6A). Quantitative western blot analysis in Fig. 6B using nuclear protein was also confirmed that CAP (10 nM) significantly increased content of HIF1α in nuclear protein of TRPV1-A549 cells, but not in TRPV1 siRNA pretreatment TRPV1$^{-/-}$-A549 cells. It means that HIF1α nuclear translocation in A549 cells was regulated at least in part by TRPV1.

To investigate whether nuclear translocation of HIF1α induced by TRPV1 was responsible for NOS1-NO signal pathway, calcium influx ($Ca^{2+}{}_{[i]}$), nitric oxide release, cytoplasmic nNOS, as well as nuclear HIF1α were measured. Ca^{2+} influx ($Ca^{2+}{}_{[i]}$) was recorded by Fura 2-AM probe by the fluorescence value of F340/F380. As shown in Fig. 6C, CAP (10 nM) perfusion evoked a brief but powerful $Ca^{2+}{}_{[i]}$ into TRPV1-A549 cells, which was almost blocked

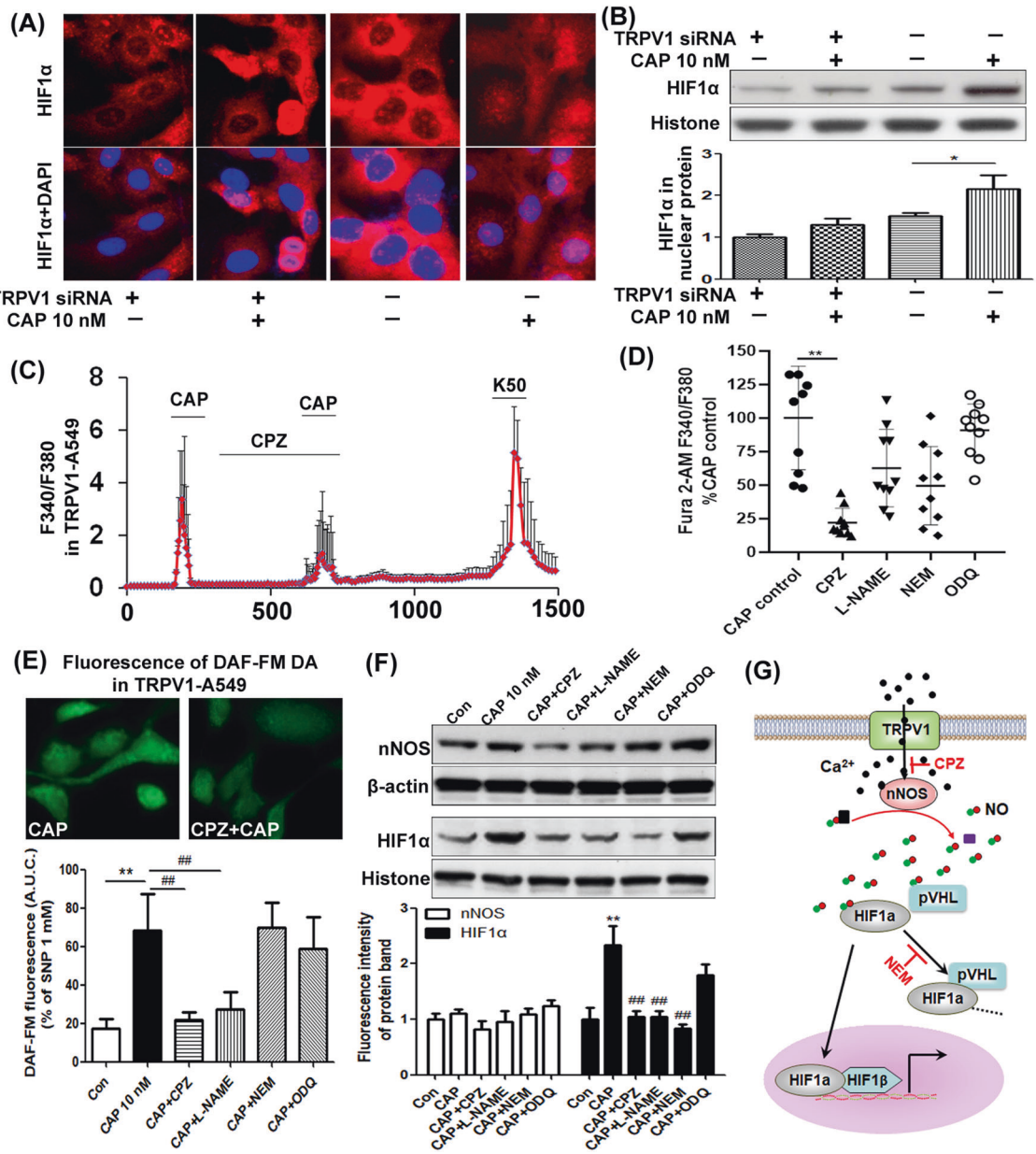

Fig. 6 TRPV1 overexpression promotes HIF1α nuclear translocation through activation of NOS1-NO pathway. Images of IFC staining (**A**) and western blot (**B**) showing nuclear translocation of HIF1α influenced by CAP (10 nM, 1 h) or TRPV1 siRNA (5 nM, for 48 h) pretreatment. **C** Calcium influx ($Ca_2^{+}{}_{[i]}$) in TRPV1-A549 cells was recorded by Fura 2-AM probe during superfusing with CAP (10 nM, for 3 min) and/or CPZ (25 μM, for 10 min pre-superfuse). **D** $Ca_2^{+}{}_{[i]}$ in TRPV1-A549 cells evoked by CAP superfusing was recorded by Fura 2-AM probe, For the compound test, Cells was pre-superfused with CPZ (25 μM), L-NAME (25 μM), NEM (25 μM), or ODQ (25 μM) for 10 min, and then superfused with solutions containing CAP (10 nM) for 3 min. **E** Nitrc oxide production in TRPV1-A549 cells after 1 h incubation with CAP (10 nM), CPZ (25 μM), LNAME (25 μM), NEM (25 μM), or ODQ (25 μM) was measured by DAF-FM DA probe. **F** Cytoplasmic nNOS and nuclear translocation of HIF1α were detected by Western blot. **G** Proposed mechanism and signal pathway involved in TRPV1-induced HIF1α nuclear translocation. Data were expressed as Mean ± SEM ($n = 3$). *Represents significant difference as compared with control group, $^{*}p < 0.05$, $^{**}p < 0.01$. $^{\#}$ Represents significant difference as compared with CAP group, $^{\#}p < 0.05$, $^{\#\#}p < 0.01$.

by CPZ (25 μM) pretreatment. As shown in Fig. 6D, $Ca^{2+}{}_{[i]}$ in TRPV1-A549 cells evoked by CAP was mildly inhibited by LNAME (25 μM) or NEM (25 μM) pretreatment, but not by ODQ (25 μM) pretreatment. NO release, measured by DAF-FM DA probe, demonstrated that CAP (10 nM) incubation for 5 min induced NO production in TRPV1-A549 cells, which was significantly inhibited by both CPZ (25 μM) and LNAME (25 μM) pretreatment, but not by NEM (25 μM) or ODQ (25 μM) pretreatment (Fig. 6E). Moreover, pretreatment with any of the three drugs (LNAME, NEM, and CPZ) significantly reduced the content of HIF1α in the nucleus of TRPV1-A549 cells (Fig. 6F). These results indicated that TRPV1 overexpression promotes HIF1α nuclear translocation by upregulating nNOS-NO signal pathway.

CuS-TRPV1 mAb photothermal nanoparticles reverse TRPV1-induced growth and invasion both in vitro and in vivo

Here, we used photothermal nanoparticles CuS-TRPV1 mAb to accurately target tumor cells showing high level TRPV1 expression, followed by induction of apoptosis by the photothermal effect of CuS. TRPV1 (green fluorescence) was only detected in TRPV1-A549

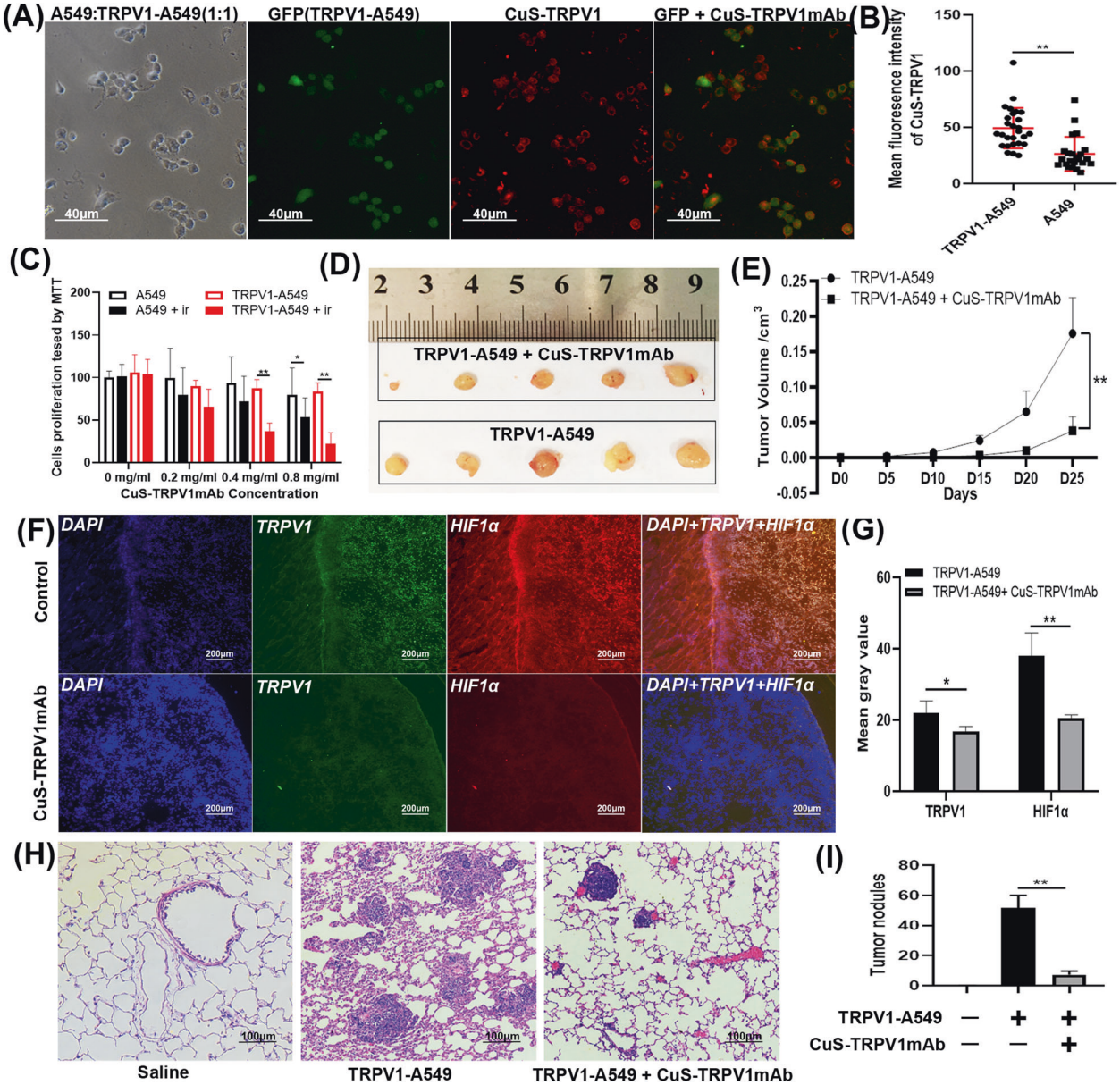

Fig. 7 CuS-TRPV1 mAb photothermal nanoparticles reverse TRPV1-induced growth and invasion both in vitro and in vivo. Absorption (**A**) and quantitative analysis (**B**) of photothermal nanoparticles CuS-TRPV1 mAb (0.4 mg mL^{-1}) in A549 cells and TRPV1-A549 cells. (**C**) The proliferation of A549 or TRPV1-A549 cells influenced by CuS-TRPV1 mAb before or after exposure of the cells to the laser for 30 s (980 nm, 1 W cm^{-2}), was detected by MTT assay. (**D**) Subcutaneous tumors harvested from BALB/c nude mice transplanted with TRPV1-A549 cells or CuS-TRPV1 mAb-pretreated TRPV1-A549 cells. (**E**) Tumor volume changes after TRPV1-A549 cells transplantation and CuS-TRPV1 mAb treatment. The expression (**F**) and quantitative analysis (**G**) of TRPV1 and HIF1α in subcutaneous tumors. (**H**) H&E staining showing metastatic nodules of systemic metastasis established by tail vein injection of TRPV1-A549 cells or CuS-TRPV1 mAb pretreatment of TRPV1-A549 cells. (**I**) Quantitative number of metastatic nodules induced by the TRPV1-A549 or CuS-TRPV1 mAb pretreatment of TRPV1-A549 cells 35 days after tail vein injection. Data were expressed as Mean ± SEM ($n = 5$). *Represents significant difference as compared with control group, *$p < 0.05$, **$p < 0.01$.

cells, but red fluorescence showing CuS-TRPV1 mAb was seen on the membrane of both TRPV1-A549 cells and A549 cells after 2 h incubation with CuS-TRPV1 mAb (0.4 mg mL^{-1}). The mean fluorescent density (MFI) of CuS-TRPV1 mAb on TRPV1-A549 cells was significantly higher than that on the membrane of A549 cells (49.3 ± 18.1 versus 26.4 ± 15.2; $P < 0.01$; Fig. 7A, B). To investigate the in vitro cytotoxicity of CuS-TRPV1 mAb on TRPV1-A549 cells and A549 cells, several doses of CuS-TRPV1 mAb with concentration gradient (0, 0.2, 0.4, 0.8 mg mL^{-1}) were added into cell culture medium for 4 h incubation. Fresh medium was then provided and the cells were exposed to the laser for 30 s (980 nm, 1 W cm^{-2}). CuS-TRPV1 mAb exhibited an overall higher cytotoxicity to TRPV1-A549 cells than to normal A549 cells, which could be attributed to direct laser excitation, as the unexcited CuS-TRPV1 mAb showed no cytotoxicity to both TRPV1-A549 cells and A549 cells (Fig. 7C).

In vivo, CuS-TRPV1 mAb pretreate d TRPV1-A549 cells produced significantly smaller tumors than untreated TRPV1-A549 cells (Figs. 7D and 3E). Tumors derived from CuS-TRPV1 mAb treated TRPV1-A549 cells exhibited significantly lower levels of both TRPV1 and HIF1α staining, compared with tumors from untreated TRPV1-A549 cells (Fig. 7F, G).

In the in vivo metastasis model, the number of lung metastatic nodules was significantly reduced in the CuS-TRPV1 mAb pretreated TRPV1-A549 group, compared with the untreated

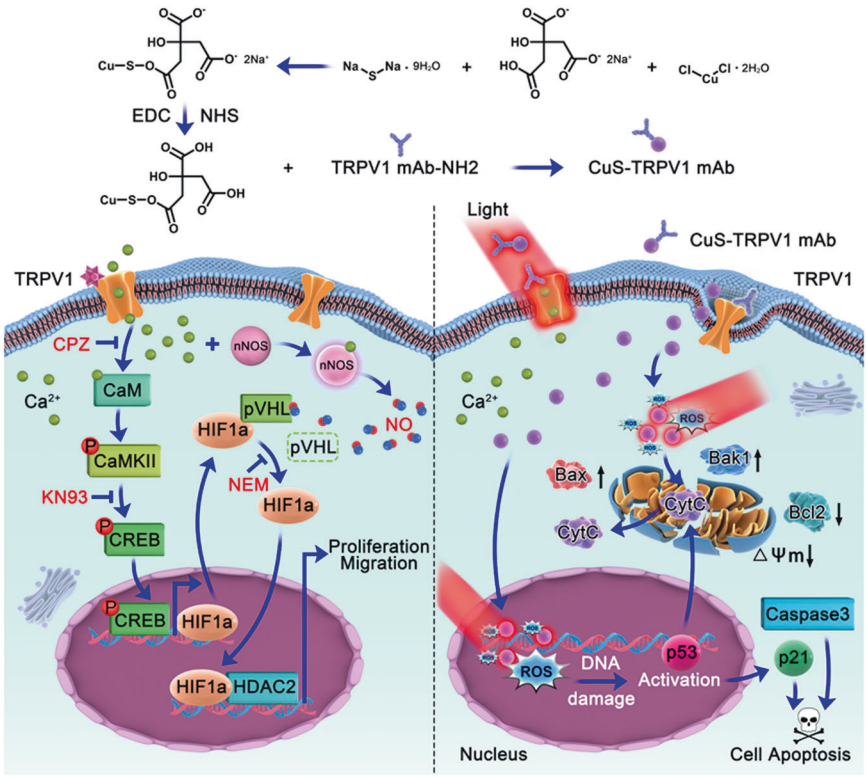

Fig. 8 Schematic of the role of TRPV1 in growth and invasion of LUAD tumors, which be reversed by CuS-TRPV1 mAb photothermal nanoparticles. In LUAD tumor cells, TRPV1 mediates activation of HIF1α resulting in enhanced proliferation and metastatic rate of tumor cells. CuS-TRPV1 mAb reversed the proliferation and invasive process of TRPV1-A549 cells and reduced HIF1α expression level in xenograft tumors of BALB/c nude mice.

TRPV1-A549 group (7.2 ± 2.5 versus 51.6 ± 8.4; $P < 0.01$; Fig. 7H, I). These results indicated that CuS-TRPV1 mAb pretreatment reverses the growth and metastasis of tumor xenografts from TRPV1-A549 cells in BALB/c nude mice.

DISCUSSION

In the present study, four key findings were obtained regarding to the role of TRPV1 in the proliferation and invasion of LUAD tumor cells. Firstly, TRPV1 expression was positively correlated with the malignancy of LUAD. Secondly, TRPV1 overexpression enhanced the proliferation and invasion ability of NSCLC cells. Thirdly, the promoted proliferation and invasion of NSCLC cells induced by TRPV1 were mediated by HIF1α activation through nNOS-NO pathway and calcium influx release. Fourthly, CuS-TRPV1 mAb reversed the proliferation and invasive process of TRPV1-A549 cells and reduced HIF1α expression level in xenograft tumors of BALB/c nude mice (Fig. 8).

TRPV1 is an important cationic channel, which plays an important role in mediating pain [30] and cough [31]. The expression of TRPV1 varies in different types of tumors, for example high level expression in cervical cancer (CC) [32] and breast cancer [33], and low leve expression in renal cell carcinoma (RCC) [34] and gastric cancer [35]. Previous studies have suggested that TRPV1 mainly mediates tumor-related pain in patients with cancers [36], but few studies have reported the relationship between TRPV1 and the clinical course and malignant phenotype of cells [20]. In the present study, we confirmed that tumor cells with overexpressed TRPV1 were indeed involved in the metastasis of LUAD. Therefore, it is plausible to suggest that where there is a higher TRPV1 expression in a particular cancer type, the TRPV1 overexpressing tumor cells manifest stronger invasiveness. Moreover, in the present study, we not only confirmed that TRPV1 overexpression promoted metastasis, but also confirmed that TRPV1 plays the above role by activating HIF1α. Our previous study confirmed that TRPV1 expression would be upregulated after HIF1α activation [19]. Together, this would indicate a cross talk between TRPV1 and HIF1α, which synergistically promoted recurrence and development of LUAD.

Here, the newly discovered mechanism further led us to reveal that photothermal nanoparticles CuS-TRPV1 mAb, which targeted to TRPV1, precisely killed tumor cells with TRPV1 over-expression, thereby inhibited tumor proliferation and metastasis. Gao et al. previously confirmed CuS-TRPV1 mAb nanoparticles as a photothermal switch for TRPV1 signaling to locally and temporally impede foam cell formation and then attenuate atherosclerosis [29]. Our newly synthesized CuS-TRPV1 mAb has targeting selectivity to TRPV1-A549 cells. However, the photothermal cytotoxicity to the TRPV-1 expressing cancer cells appears to be more prominent than targeting itself [37, 38]. Thus, we speculate that CuS-TRPV1 mAb is a stone killing two birds: molecular targeting and targeted cytotoxicity, an exciting feature for therapeutic consideration. Our data strongly suggested that CuS-TRPV1 mAb achieved cytotoxicity, by generating free radicals through the photothermal effect of CuS [37] and activating calcium influx through the thermally-opened TRPV1 to further induce calcium overload. TRPV1 when over-expressed in tumor cells renders the cells with strong invasiveness. Thus, targeting and precisely killing these cells by TRPV1-targeted CuS or any other photothermal nanoparticles such as Fe(III) and cypate [38] may also contribute to inhibit tumor recurrence. On the other hand, TRPV1 has been recognized to mediate tumor-related pain [30, 36]. CuS-TRPV1 mAb intervention would also alleviate TRPV1-mediated tumor-related pain, which may also have clinical benefits.

Although the results in the present study confirmed that CuS-TRPV1 mAb showed a certain therapeutic value in inhibiting the proliferation and invasion of TRPV1-A549 cells, there are several hurdles needed to be overcome before its consideration for clinical application. Firstly, CuS is irradiated at 980 nm, the wavelength of near-infrared light does not penetrate tissues of deep layer. Therefore, in the present study, TRPV1-A549 cells are treated with CuS-TRPV1 mAb in vitro first and then injected into the tail vein. Secondly, alternative photothermal materials, that are more suitable for clinical application than CuS, can be considered. Given that the metabolism of CuS in vivo remains unclear, new photothermal molecules with better light penetration and biological metabolism, such as black phosphorus [39] and indocyanine green [40], may be applied to the targeted photothermal therapy of LUAD. Thirdly, considering the huge molecular weight of TRPV1 antibody, it would be attractive to construct nanomaterials by only preserving the fragments of key recognition sequences of TRPV1 mAb [41]. In most traditional cancer therapies such as chemotherapies, drugs are systemically reaching the whole body and/or radiotherapy, which targets all the tissues/organs indiscriminately in the path of the radiation. The method we developed here targeted to the specific molecule and location. This novel approach affords opportunity to reduce the side effects and collateral damages, arguably presenting a potentially promising way to combine with surgery. Sonodynamic therapy, developed on the basis of photodynamic therapy, is able to penetrate to deep tissue due to activation of ultrasound and overcomes the penetration limitations of light [42], would be an attractive option in the future.

CONCLUSIONS

TRPV1 hyperexpression in LUAD is a risk factor for tumor progression. TRPV1 hyperexpression increased the proliferation and migration of tumor cells through activation of HIF1α. CuS-TRPV1 mAb may selectively target and precisely kill TRPV1 hyperexpression cells through antibody and photothermal effects, thereby inhibiting the recurrence and metastasis of LUAD cancer cells.

DATA AVAILABILITY

All data, models, and code generated or used during the study appear in the submitted article.

REFERENCES

1. He ZH, Lv W, Wang LM, Wang YQ, Hu J. Identification of genes associated with lung adenocarcinoma prognosis. Comb Chem High Throughput Screen. 2019;22:220–4.
2. Yang CY, Yang JC, Yang PC. Precision management of advanced non-small cell lung cancer. Annu Rev Med. 2020;71:117–36.
3. Paez JG, Jänne PA, Lee JC, Tracy S, Greulich H, Gabriel S, et al. EGFR mutations in lung cancer: correlation with clinical response to gefitinib therapy. Science. 2004;304:1497–500.
4. Muller IB, de Langen AJ, Giovannetti E, Peters GJ. Anaplastic lymphoma kinase inhibition in metastatic non-small cell lung cancer: clinical impact of alectinib. Onco Targets Ther. 2017;10:4535–41.
5. Kwak EL, Bang YJ, Camidge DR, Shaw AT, Solomon B, Maki RG, et al. Anaplastic lymphoma kinase inhibition in non-small-cell lung cancer. N. Engl J Med. 2010;363:1693–703.
6. Drilon A, Wang L, Hasanovic A, Suehara Y, Lipson D, Stephens P, et al. Response to Cabozantinib in patients with RET fusion-positive lung adenocarcinomas. Cancer Discov. 2013;3:630–5.
7. Bergethon K, Shaw AT, Ou SH, Katayama R, Lovly CM, McDonald NT, et al. ROS1 rearrangements define a unique molecular class of lung cancers. J Clin Oncol. 2012;30:863–70.
8. Liu Y, Gao GF, Minna JD, Williams NS, Westover KD. Loss of wild type KRAS in KRASMUT lung adenocarcinoma is associated with cancer mortality and confers sensitivity to FASN inhibitors. Lung Cancer. 2021;153:73–80.
9. Ou SH, Kwak EL, Siwak-Tapp C, Dy J, Bergethon K, Clark JW, et al. Activity of crizotinib (PF02341066), a dual mesenchymal-epithelial transition (MET) and anaplastic lymphoma kinase (ALK) inhibitor, in a non-small cell lung cancer patient with de novo MET amplification. J Thorac Oncol. 2011;6:942–6.
10. Shukuya T, Carbone DP. Predictive Markers for the Efficacy of Anti-PD-1/PD-L1 Antibodies in Lung Cancer. J Thorac Oncol. 2016;11:976–88.
11. Chen L, Han X. Anti-PD-1/PD-L1 therapy of human cancer: past, present, and future. J Clin Invest. 2015;125:3384–91.
12. He Y, Jiang Z, Chen C, Wang X. Classification of triple-negative breast cancers based on Immunogenomic profiling. J Exp Clin Cancer Res. 2018;37:327.
13. Bujak JK, Kosmala D, Szopa IM, Majchrzak K, Bednarczyk P. Inflammation, Cancer and Immunity-Implication of TRPV1 Channel. Front Oncol. 2019;9:1087.
14. Benítez-Angeles M, Morales-Lázaro SL, Juárez-González E, Rosenbaum T. TRPV1: structure, endogenous agonists, and mechanisms. Int J Mol Sci. 2020;21:3421.
15. Hurtado-Zavala JI, Ramachandran B, Ahmed S, Halder R, Bolleyer C, Awasthi A, et al. TRPV1 regulates excitatory innervation of OLM neurons in the hippocampus. Nat Commun. 2017;8:15878.
16. Hou N, He X, Yang Y, Fu J, Zhang W, Guo Z, et al. TRPV1 induced apoptosis of colorectal cancer cells by activating calcineurin-NFAT2-p53 signaling pathway. Biomed Res Int. 2019;2019:6712536.
17. Dietrich A. Modulators of transient receptor potential (TRP) channels as therapeutic options in lung disease. Pharm (Basel). 2019;12:23.
18. Zhu YF, Wu SB, Zhou MQ, Xie MR, Xiong R, Xu SB, et al. Increased expression of TRPV1 in patients with acute or chronic cough after lung cancer surgery. Thorac Cancer. 2019;10:988–91.
19. Nie Y, Huang C, Zhong S, Wortley MA, Luo Y, Luo W, et al. Cigarette smoke extract (CSE) induces transient receptor potential ankyrin 1(TRPA1) expression via activation of HIF1αin A549 cells. Free Radic Biol Med. 2016;99:498–507.
20. Lozano C, Córdova C, Marchant I, Zúñiga R, Ochova P, Ramírez-Barrantes R, et al. Intracellular aggregated TRPV1 is associated with lower survival in breast cancer patients. Breast Cancer (Dove Med Press). 2018;10:161–8.
21. Omari SA, Adams MJ, Geraghty DP. TRPV1 Channels in immune cells and hematological malignancies. Adv Pharmacol. 2017;79:173–98.
22. Haga RB, Ridley AJ. Rho GTPases: Regulation and roles in cancer cell biology. Small GTPases. 2016;7:207–21.
23. Brüne B, Zhou J. The role of nitric oxide (NO) in stability regulation of hypoxia inducible factor-1alpha (HIF-1alpha). Curr Med Chem. 2003;10:845–55.
24. Li J, Zhang JT, Jiang X, Shi X, Shen J, Feng F, et al. The cystic fibrosis transmembrane conductance regulator as a biomarker in non-small cell lung cancer. Int J Oncol. 2015;46:2107–15.
25. Li J, Ye L, Shi X, Chen J, Feng F, Chen Y, et al. Repulsive guidance molecule B inhibits metastasis and is associated with decreased mortality in non-small cell lung cancer. Oncotarget. 2016;7:15678–89.
26. Li J, Ye L, Sanders AJ, Jiang WG. Repulsive guidance molecule B (RGMB) plays negative roles in breast cancer by coordinating BMP signaling. J Cell Biochem. 2012;113:2523–31.
27. Agrawal S, Kumari R, Luthra PM. A reliable fluorimetric method to screen the nitric oxide synthase inhibitors in 96 well plate. Anal Biochem. 2019;577:42–4.
28. Bonvini SJ, Birrell MA, Dubuis E, Adcock JJ, Wortley MA, Flajolet P, et al. Novel airway smooth muscle-mast cell interactions and a role for the TRPV4-ATP axis in non-atopic asthma. Eur Respir J. 2020;56:1901458.
29. Gao W, Sun Y, Cai M, Zhao Y, Cao W, Liu Z, et al. Copper sulfide nanoparticles as a photothermal switch for TRPV1 signaling to attenuate atherosclerosis. Nat Commun. 2018;9:231.
30. Frias B, Merighi A. Capsaicin, nociception and pain. Molecules. 2016;21:797.
31. Belvisi MG, Birrell MA, Wortley MA, Maher SA, Satia I, Badri H, et al. XEN-D0501, a novel transient receptor potential vanilloid 1 antagonist, does not reduce cough in patients with refractory cough. Am J Respir Crit Care Med. 2017;196:1255–63.
32. Han GH, Chay DB, Nam S, Cho H, Chung JY, Kim JH. The combination of transient receptor potential vanilloid type 1 (TRPV1) and phosphatase and tension homolog (PTEN) is an effective prognostic biomarker in cervical cancer. Int J Gynecol Pathol. 2021;40:214–23.
33. So CL, Milevskiy MJG, Monteith GR. Transient receptor potential cation channel subfamily V and breast cancer. Lab Invest. 2020;100:199–206.
34. Wu YY, Liu XY, Zhuo DX, Huang HB, Zhang FB, Liao SF. Decreased expression of TRPV1 in renal cell carcinoma: association with tumor Fuhrman grades and histopathological subtypes. Cancer Manag Res. 2018;10:1647–55.
35. Gao N, Yang F, Chen S, Wan H, Zhao X, Dong H. The role of TRPV1 ion channels in the suppression of gastric cancer development. J Exp Clin Cancer Res. 2020;39:206.
36. Zhang S, Zhao J, Meng Q. AAV-mediated siRNA against TRPV1 reduces nociception in a rat model of bone cancer pain. Neurol Res. 2019;41:972–9.
37. Yang C, Ma L, Zou X, Xiang G, Chen W. Surface plasmon-enhanced Ag/CuS nanocomposites for cancer treatment. Cancer Nanotechnol. 2013;4:81–9.

38. Yin Y, Li Y, Wang S, Dong Z, Liang C, Sun J, et al. MSCs-engineered biomimetic PMAA nanomedicines for multiple bioimaging-guided and photothermal-enhanced radiotherapy of NSCLC. J Nanobiotechnology. 2021;19:80.
39. Wang S, Shao J, Li Z, Ren Q, Yu XF, Liu S. Black phosphorus-based multimodal nanoagent: showing targeted combinatory therapeutics against cancer metastasis. Nano Lett. 2019;19:5587–94.
40. Hirohashi K, Anayama T, Wada H, Nakajima T, Kato T, Keshavjee S, et al. Lung cancer photothermal ablation by low-power near-infrared laser and topical injection of indocyanine green. Interact Cardiovasc Thorac Surg. 2019;29:693–8.
41. Schmid D, Park CG, Hartl CA, Subedi N, Cartwright AN, Puerto RB, et al. T cell-targeting nanoparticles focus delivery of immunotherapy to improve antitumor immunity. Nat Commun. 2017;8:1747.
42. Son S, Kim JH, Wang X, Zhang C, Yoon SA, Shin J, et al. Multifunctional sonosensitizers in sonodynamic cancer therapy. Chem Soc Rev. 2020;49:3244–61.

ACKNOWLEDGEMENTS

This study was supported by the project of Pearl River Nova Program of Guangzhou (No. 201806010008), the project of "Dengfeng Plan" High-level Hospital Construction Opening Project of Foshan Fourth People's Hospital (No. FSSYKF-2020010), the National Natural Science Foundation of China (81672270), the Natural Science Foundation of Guangdong Province, China (2020KZDZX1160), the Autonomous Foundation of the State Key Laboratory of Respiratory Diseases (SKLRD-QN-201907,SKLRD2016ZJ017), the Opening Foundation of the State Key Laboratory of Respiratory Diseases (SKLRD-OP-201915). The funders had no role in the planning or execution of this study or the preparation of this manuscript. Thanks the Biobank for Respiratory Diseases in the National Clinical Research Center for Respiratory Disease (BRD-NCRCRD, Guangzhou, Southern China). Dr. Andres J Sanders was supported by a RealCan Fellowship. The authors wish to thank Dr. Jane Lane for critically reading the manuscript.

AUTHOR CONTRIBUTIONS

YCN, FLF, and JL involved in the study concept and design; LJZ, WL, JC, JL, and WNF provided samples and clinical data; YDZ provided the CuS-TRPV1 mAb; YCN, CC, and WW performed experiments related to in vitro cells and molecular biology; AJS, FLF and JML performed experiments related to clinical cohorts experiments, clinical data analysis and in vivo animal models. WQG and WPL performed statistical analysis; YCN, JL, and WGJ designed study, performed experiments, data collection, data analysis and drafted the manuscript. All authors read and approved the final manuscript.

COMPETING INTERESTS

The authors declare no competing interests.

ADDITIONAL INFORMATION

Supplementary information The online version contains supplementary material available at https://doi.org/10.1038/s41417-022-00459-0.

Correspondence and requests for materials should be addressed to Jin Li.

Reprints and permission information is available at http://www.nature.com/reprints

Publisher's note Springer Nature remains neutral with regard to jurisdictional claims in published maps and institutional affiliations.